GEOMAGNETIC INVESTIGATIONS IN THE PINGTUNG PLAIN, TAIWAN

by Shui-Beih Yu and Yi-Ben Tsai

ABSTRACT

A magnetic survey was carried out in the Pingtung plain in the winter of 1978. Two portable proton magnetometers of 1 gamma sensitivity were used to measure the total geomagnetic field intensity. The residual magnetic intensity map was prepared by removing the first-degree trend surface values from the diurnally corrected total intensity values. Two prominent features of the magnetic anomalies can be recognized in the map. The first is the magnetic anomalies of small amplitude with an extent of only a few kilometers scattered over the entire plain. They are considered to be caused by local variations of mangetic susceptibility of near-surface sedimentary rocks or by the cultural disturbances from nearby towns and industrial districts. The second is the large-area magnetic anomaly of low amplitude which may be due to deeper basement rocks. The linear secular variation predicted by IGRF 1975 is compared with the observed geomagnetic data at Lunping observatory in northwestern Taiwan. It is found that the observed values of secular change generally fall within several gammas by the IGRF 1975 line during the period from 1965 to 1973. On the contrary, the data acquired after the epoch 1974 clearly form an increasing trend as opposed to the decreasing IGRF 1975 line. We also find that in the case of Pingtung plain the first-degree trend surface of total intensity is more suitable to represent the regional field of the plain than the IGRF contours. Finally, the magnetic anomalies of the plain are reduced to the north magnetic pole of the earth by utilizing the fast Fourier transorm technique. Also the magnetic basement relief of the plain is estimated by doing the downward continuation through the pseudo-gravity anomalies.

INTRODUCTION

The Pingtung[1] plain in southern Taiwan is approximately rectangular in shape. It is surrounded by low hills in the north and west sides, and by the wall-like southern stretch of the Central Range in the east (Figure 1). This plain extends southward to the southwest coast of Taiwan. Its topography is generally flat and slopes down from the northeast. The eastern part of the plain is covered by a series of alluvial fans (Hsu, 1961). The Kaopinghsi[2], the largest stream flowing through the plain, has played an important role in the accumulation of recent sediments in this area.

In order to study the subsurface structures of the Pingtung plain, a detailed gravity survey as well as an extensive seismic survey were carried out in this area by the Taiwan Petroleum Exploration Division, Chinese Petroleum Corporation in the past. Combining these valuable geophysical data with geologic information, Pan (1969) and Hsieh (1970) inferred the subsurface geologic structures of the plain. Since geomagnetic data may improve our understanding of the plain's subsurface structure and of the geomagnetic features of this area, a detailed magnetic survey was conducted by the Institute of Earth Sciences (Preparafory Office), Academia Sinica from November 1978 to February 1979. This survey covered an area of about 1400 km^2, extending from Maolin[3] and Fangliao[4] in the east to Yenchao[5] and

1. 屏東 2. 高屏溪 3. 茂林 4. 枋寮 5. 燕巢

Fengshan[6] in the west, and from Chishan[7] and Meinung[8] in the north to seacoast in the south.

In this paper the results of this magnetic survey are presented. Also the applicability of the International Geomagnetic Reference Field (IGRF) in reducing the geomagnetic survey data of Taiwan region is reviewed. The fast Fourier transform technique is utilized to reduce the total magnetic intensity anomalies of the Ping-

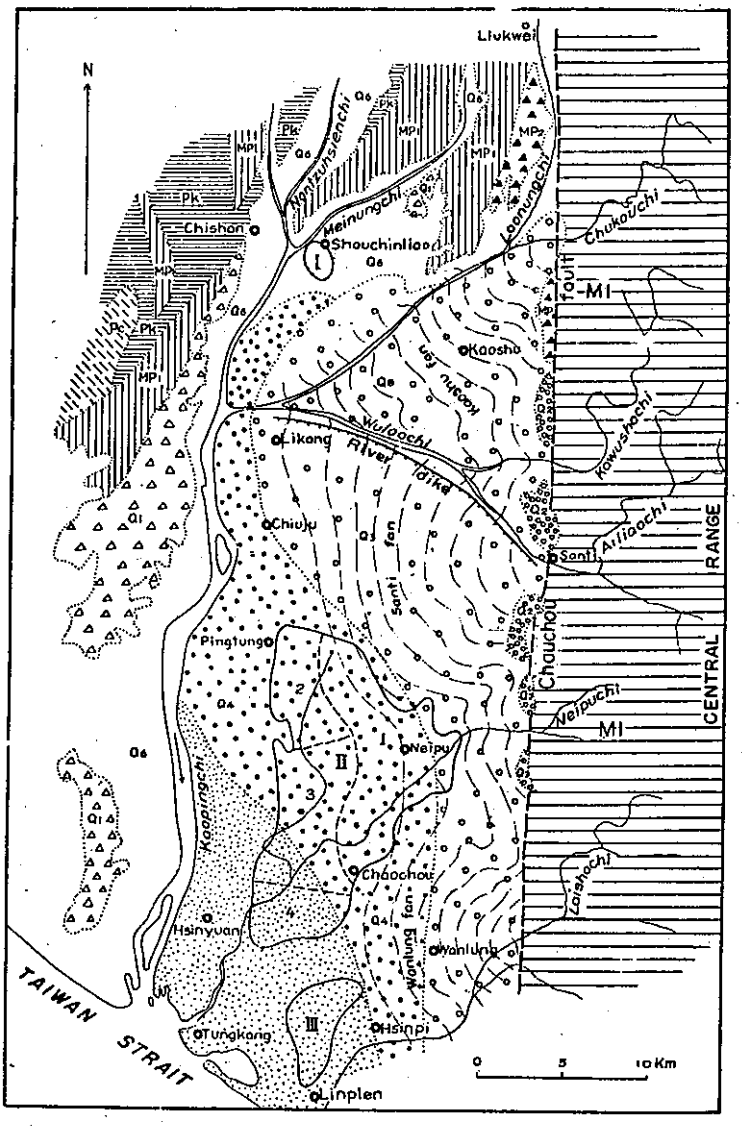

Figure 1. Geological map of the Pingtung region (after Hsu, 1961). Q6, alluvium undifferentiated; Q5, silt, clay, and some sand; Q4, alternating layers of gravel, sand, silt, and clay; Q3, coarse gravel; Q1, Lingkou conglomerate, P_C, Chi.ing formation; P_K, Kutingkeng formation, MP2, conglomerate of Mucha formation; MP1, sandstone and shale of Mucha formation, M1, Lushan formation.

6. 鳳山 7. 旗山 8. 美濃

tung plain to the magnetic pole of the earth. The relief of magnetic basement of the plain is estimated by performing the downward continuation through the pseudo-gravity anomalies.

GEOLOGICAL SETTING

The general geology of the Pingtung plain and its surrounding mountainous region is shown in Figure 1 (Hsu, 1961). The plain is covered with unconsolidated alluvial deposits of clay, sands, and gravels of Recent age, while Neogene rocks are ditributed around the border of the plain.

The Lushan[9]formation of Miocene age is distributed on the western flank of the Central Range that borders the east of the plain. It is a thick sequence of black slate intercalated with beds of coarse- or fine-grained quartzose sandstone. Rocks cropping out in the region north of the plain is the Mio-Pliocene Mucha[10] formation. The lower part of this formation is composed mainly of sandstone and shale and having a thickness of about 3000 m. The upper part of the formation is a 1000 m thick conglomerate. The Pliocene Kutingkeng[11] formation is exposed widely in the northwest of the Pingtung plain. It consists chiefly of sandy shale and with beds of shale and sandstone. Its thickness ranges from 1600 to 1800 m. Also exposed in the northwest of the plain is the Chiting[12] formation of Pliocene age. It attains a thickness of 1800 m, the lower 400 m of which is mainly of shaly sandstone and the upper 1400m of sandstone with some shale and sandy shale. The Pleistocene Lingkou[13] conglomerate is a loose deposit, about 3000 m thick, cropping out as a narrow strip along the western edge of the plain. It is unconformably overlain by terrace gravel.

After analyzing the gravity anomaly data obatined from a detailed gravity survey together with geologic information, Hsieh (1970) suggested the following structural elements in the Pingtung plain (Figure 2):

1. Pingtung basin; 2. Chaochou[14] fault; 3. Chaochou structure; 4. Liukwei[15] graben; 5. Chishan fault; 6. Fengshan anticline

The Pingtung basin is located in the central part of the plain. It is a sedimentary trough filled with low density sediments of considerable thickness. The Pingtung syncline and the Pingtung anticline are the striking features indicated by the gravity anomalies in the central part of the basin. The Chaochou fault, lying in the eastern margin of the plain, is a N-S trending high-angle thrust fault which brings the Miocene Lushan formation in direct contact with the conglomerate member of the Mucha formation in the north of the plain. The thick alluvium in the plain covers the southern stretch of this fault but we can recognize its trace from the topographic expressions and the crowding of Bouguer gravity contours along the straight eastern edge of the plain.

The Chaochou structure, located 7 km southeast of Chauchou city, is considered to be an faulted anticlinal structure. The Liukwei graben located at the northeastern corner of the Pingtung plain is a narrow small negative anomaly of about 2 milligals between the Chaochou and the Liukwei faults.

The Chishan fault is an thrust fault with the up-throw on the east side. It is traceable from Chishan to a little town Kengkou from surface geological features and is concealed by the alluvial deposits near Kengkou. The continuous gravity features corresponding closely with the trends of the Chishan fault indicate that the fault

9.廬山 10.木柵 11.古亭坑 12.崎頂 13.林口 14.潮州 15.六龜

extends further south from Kengkou to the north end of the surface axis of the Fengshan anticline. The Fengshan anticline situated on the west margin of the Pingtung plain is a broad gentle fold. It is an asymmetrical elongated anticline trending N-S with a traceable length of about 14 km and a width of 4 km. The positive anomaly produced by the deeper structrue of the anticline trends N45°E, quite different from the N-S trending of the surface axis of the anticline.

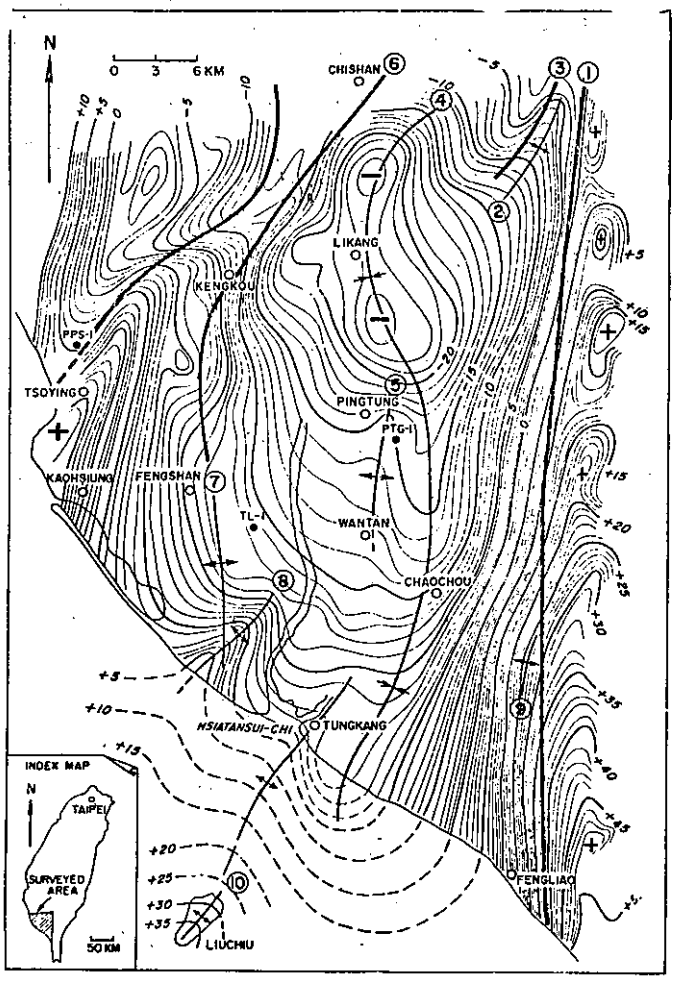

Figure 2. Bouguer gravity map with interpreted subsurface geological structures of the Pingtung plain (after Hsieh, 1970). (1), Chaochou fault; (2), Liukwei graben; (3), Liukwei fault, (4), Pingtung syncline; (5), Pingtung anticline; (6), Chishan fault, (7), Fengshan anticline, (8), Deeper trend of the Fengshan anticline; (9), Chaochou structure, (10), Hsiaoliuchiu anticline.

FIELD OBSERVATION AND DATA REDUCTION

Two portable proton magnetometers (GeoMetrics, Model G-826) with 1 gamma sensitivity were used to measure the total geomagnetic field intensity in the Pingtung plain. One magnetometer was kept at the base station and readings were taken every five or ten minutes to monitor the diurnal variation of the earth's magnetic field. Another magnetometer was carried by an operator to measure the total field inensity at each station. In total, measurements were made at 1040 stations. These

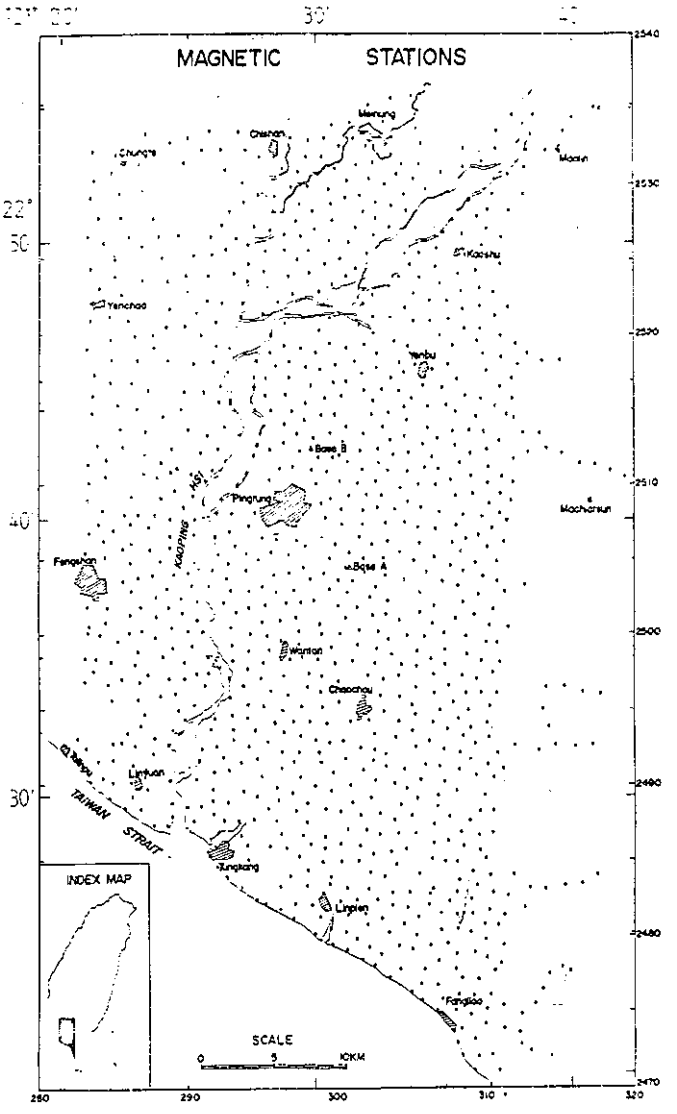

Figure 3. Distribution of the magnetic stations in the Pingtung plain.

magnetic stations were spaced about 1 to 1.5km apart (Figure 3). They were located far away from all visible or near-surface iron objects and power lines that might disturb the normal field. The locations and elevations of most stations were determined on the 1:5000 scale photographic contour maps. They were accurate enough for the present purpose so that no level and plane table surveys were required.

For convenience two magnetic base stations were employed during this survey. Base A was situated at 6 km southeast of Pingtung city (Figure 3). Base B was located at 4.5 km northeast of Pingtung city. The difference in total intensity between these two base stations has been checked to be 50 gammas. Diuranl variations in daytime were observed to range from 16 to 193 gammas. Most of them were less than 70 gammas. Several moderate magnetic disturbances occurred during the survey period.

An approximately medium value of 43,550 gammas for the total intensity values

observed at Base A was chosen as reference value and the deviations from the medium value were removed from readings at the field stations to reduce all observation data to a common datum level. Elevation corrections were made according to the expression for the vertical gradient– 0.0047 H_0 gamma/m, where H_0 is the local value of the geomagnetic field intensity in oersteds (Grant and West, 1965). Corrected total magnetic intensity contour map of the Pingtung plain was prepared at 10 gamma intervals (Figure 4).

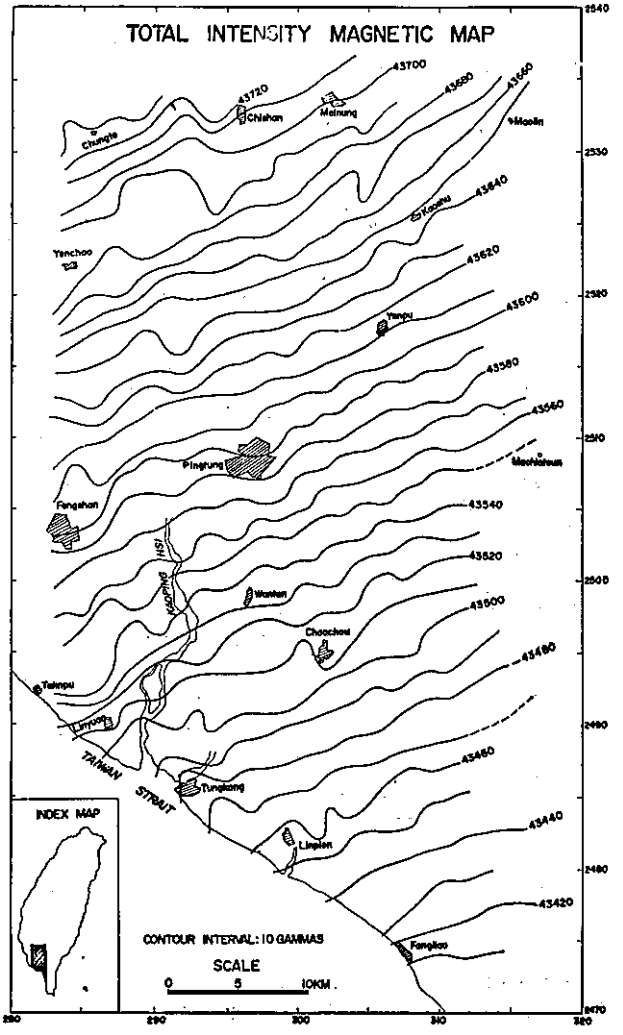

Figure 4. Corrected total magnetic intensity contour map of the Pingtung plain.

THE IGRF MODEL AND GEOMAGNETIC OBSERVATION IN TAIWAN

Accurate determination of anomalous magnetic field is important if the data are to be interpreted in terms of geologic structures. For small-scale surveys the main geomagnetic field due to the earth's core and some part of the induced field must be removed from the survey data. These components of the observed field are termed the regional field. The IGRF 1965 for the field of internal origin and its

secular variation was recommended by the International Association of Geomagnetism and Aeronomy (IAGA) Commission 2 Working Group 4 in October 1968. It is often used as the regional field in reducing survey data. But errors in the order of several ten to several hundred gammas may be introduced due to imperfect fit and inaccurate secular change correction of the IGRF model (Regan and Cain, 1975). Thus a new model (IGRF 1975) which might apply to the period 1975.0 - 1980.0 was suggested by IAGA in September 1975.

The observation program of the Lunping[16] Geomagnetic Observatory has been carried out by the Radio Wave Research Laboratories, Ministry of Communications, Republic of China, since July 1, 1965. Lunping Observatory is situated about 8 km northwest of Chungli[17] city, Taiwan. Its geographic and geomagnetic coordiantes are as follows:

Geographic Latitude	25°00N
Geographic Longitude	121° 10'E
Geomagnetic Latitude	13.8°N
Geomagnetic Longitude	189.5°E
Elevation	100m

Monthly and annual means of total magnetic field intensity for international quiet days of Lunping Observatory during the period from July 1965 to December 1978 are presented in Table 1.

Figure 5 shows the linear secular variations predicted by IGRF 1965 and IGRF 1975. For comparsion purpose in the same figure are also shown the annual means of total intensity for quiet days observed at Lunping since 1966. The observed geomagnetic field has decreased since 1965, reached the minimum value in 1973, and then reversed the trend to increase gradually. At present it increases at a rate of approximately 18 gammas per year, while the secular variation predicted by IGRF 1975 decreases at a rate of about 16 gammas per year. The secular change of the Taiwan area predicted by IGRF 1965 has been quite different from that observed at Lunping since 1965. However, Figure 5 shows clearly that IGRF 1975 fits the

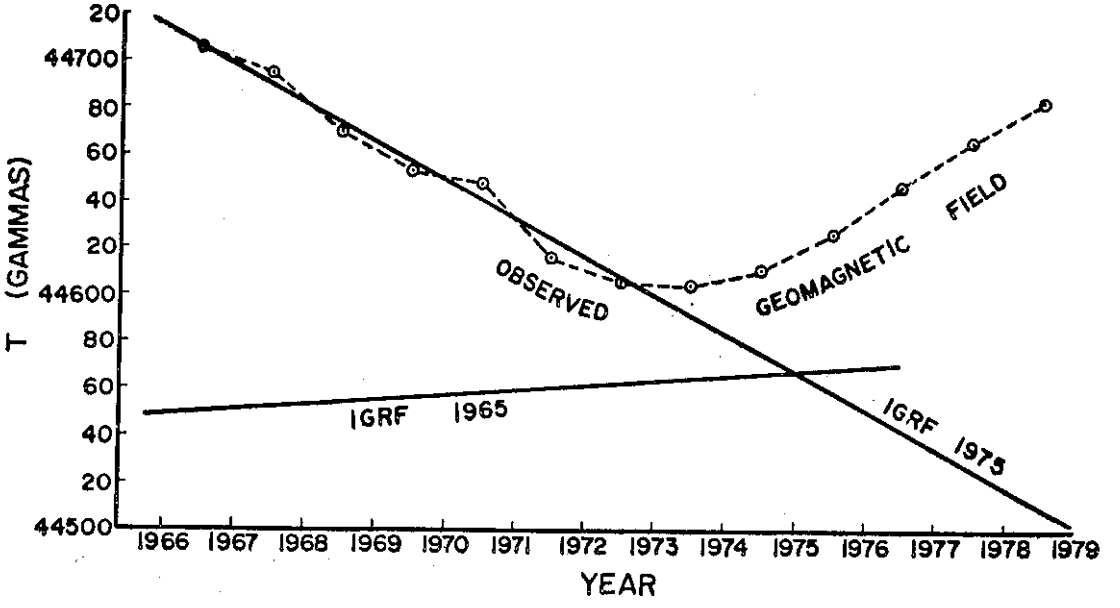

Figure 5. Comparison between the IGRF secular variation and the observed geomagnetic field at Lumping.

Table 1. Monthly and Annual Means of Total Magnetic Field for Quiet Days
(44000 + tabular values in gammas)

YEAR / MONTH	1966	1967	1968	1969	1970	1971	1972	1973	1974	1975	1976	1977	1978
JAN.	717	693	666	652	651	635	606	603	611	616	637	657	676
FEB.	716	690	671	646	657	644	606	603	610	617	641	656	675
MAR.	705	709	667	655	650	620	602	601	601	622	646	666	679
APR.	698	706	677	652	643	612	615	602	616	629	642	665	676
MAY.	709	700	677	660	651	612	611	605	611	621	646	668	681
JUN.	709	693	677	661	650	615	611	606	613	630	649	666	686
JUL.	712	699	682	668	644	614	604	610	608	628	652	670	694
AUG.	710	700	676	665	649	611	599	611	655	627	649	663	687
SEP.	686	693	663	659	651	598	602	601	607	635	642	670	686
OCT.	704	689	666	610	650	612	604	608	610	635	653	671	686
NOV.	705	693	659	650	637	609	603	604	620	628	653	679	686
DEC.	701	675	657	653	639	608	611	611	616	637	655	674	694
YEAR MEAN													

(From report of the Lunping Geomagnetic Observatory, Radio Wave Reseach Laboratories)

observed data very well in the 1966-1973 period. Thus the errors in secular change correction will be within several gammas by using IGRF 1975 to reduce the magnetic survey data in Taiwan region during the period from 1965 to 1973. For magnetic survey data obtained after the epoch 1974.0, an appropriate correction should be made if IGRF 1975 is utilized in reducing those data.

The IGRF contour chart of the Pingtung plain in the epoch 1978.9 based on IGRF 1975 is illustrated in Figure 6. The greatest horizontal gradient is 4.7 gammas

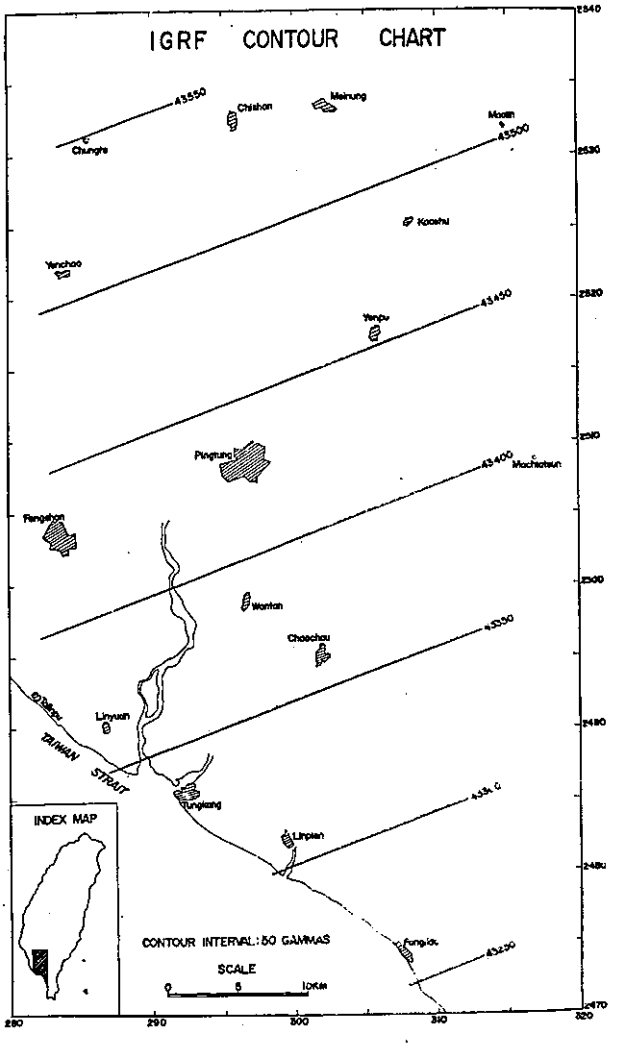

Figure 6. IGRF contour chart of the Pingtung plain.

per kilometer in N20.4°W direction. The total intensity magnetic anomaly is defined as the difference between the diurnally corrected total intensity and the IGRF value at each observation point. Since the secular change correction of IGRF 1975 is not accurate as noted previously, a value of 150 gammas was subtracted from the computed anomaly value. Figure 7 shows the corrected magnetic anomaly map of the Pingtung plain at 10 gamma contour intervals

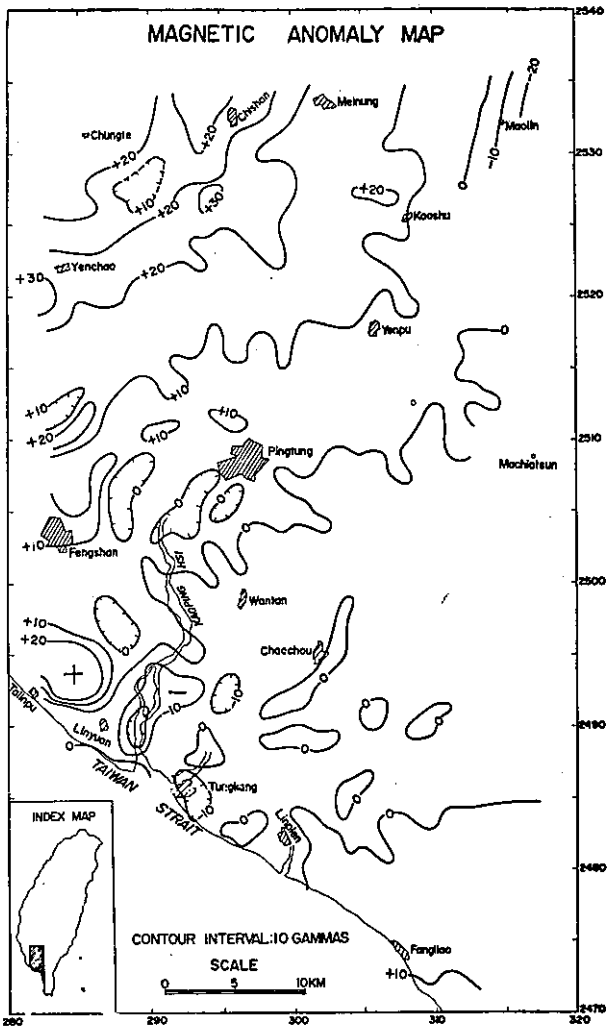

Figure 7. Corrected magnetic anomaly contour map of the Pingtung plain.

TREND-SURFACE ANALYSIS AND THE RESIDUAL MAGNETIC MAP

In order to check the validity of using the IGRF 1975 as the regional field of the study area, a trend-surface analysis of the irregularly spaced total intensity data of the area has been made. Trend-surface analysis, as practical in geology or geophysics, has invariably involved the fitting of trend surfaces to satisfy the least-squares criterion. The difference between the computed value of the trend surface at a point and the value of the observed actual surface at that point is termed the residual value. In satisfying the least-squares criterion the sum of the squared residuals is minimized. The trend surface can be thought of as the regional or large-scale component, and the residual value can be considered the local or small-scale component.

Since the magnetic stations as shown in Figure 3 are more or less evenly distributed within the studied area, so the total intensity data of the area is quite suitable for trend-surface analysis. Figure 8 shows the first-degree trend surface of total intensity of the Pingtung plain. The goodness of fit of the trend function to the

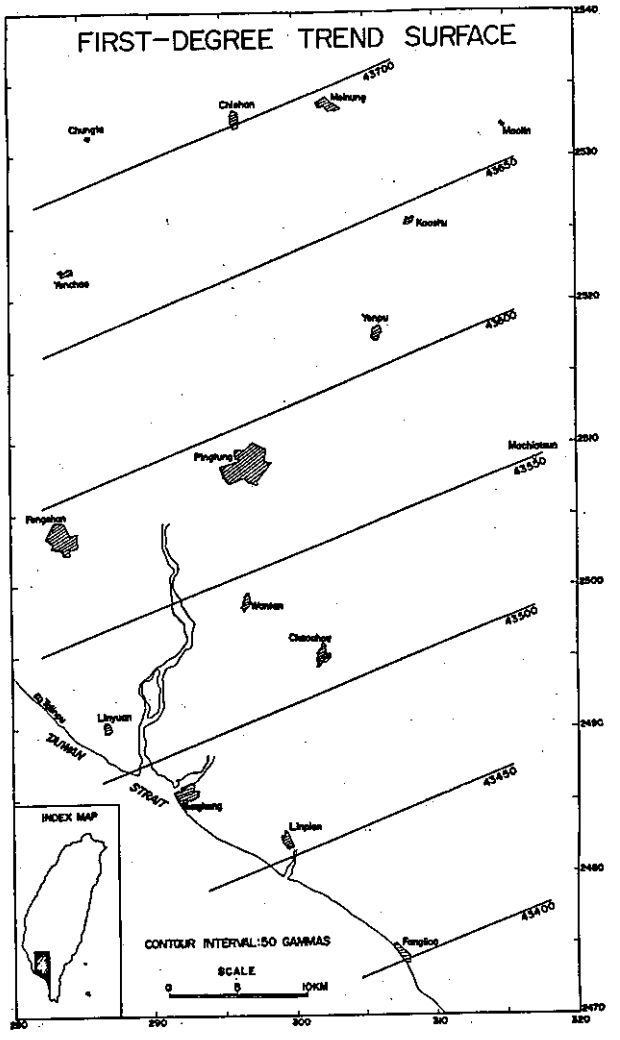

Figure 8. First-degree trend suface of total magnetic intensity of the Pingtung plain.

observed data is determined to be 97.86 percent. It means that the first-degree trend surface fits the data very well. Thus it is appropriate to take the trend surface as the regional field of the plain. The greatest horizontal gradient of the surface is 5.1 gammas per kilometer in N21°W direction. It is slightly different from that of IGRF 1975. Comparing the first-degree trend surface (Figure 8) and the IGRF contour chart (Figure 6) with the total intensity magnetic map respectively (Figure 4), it is evident that the former is more suitable for representing the regional field of the area than the latter.

The residual magnetic map of the Pingtung plain obtained by removing the trend surface values from diurnally corrected total intensity values at the observation points was prepared at 10 gamma countour intervals (Figure 9). Many small magnetic anomalies with an extent of only a few kilometers can be seen to scatter over the plain. They may be caused by local variations of magnetic susceptibility of sedimentary rocks at shallow depths or by cultural disturbances from towns and industrial districts. The positive anomaly located near Talinpu[18] is probably caused by

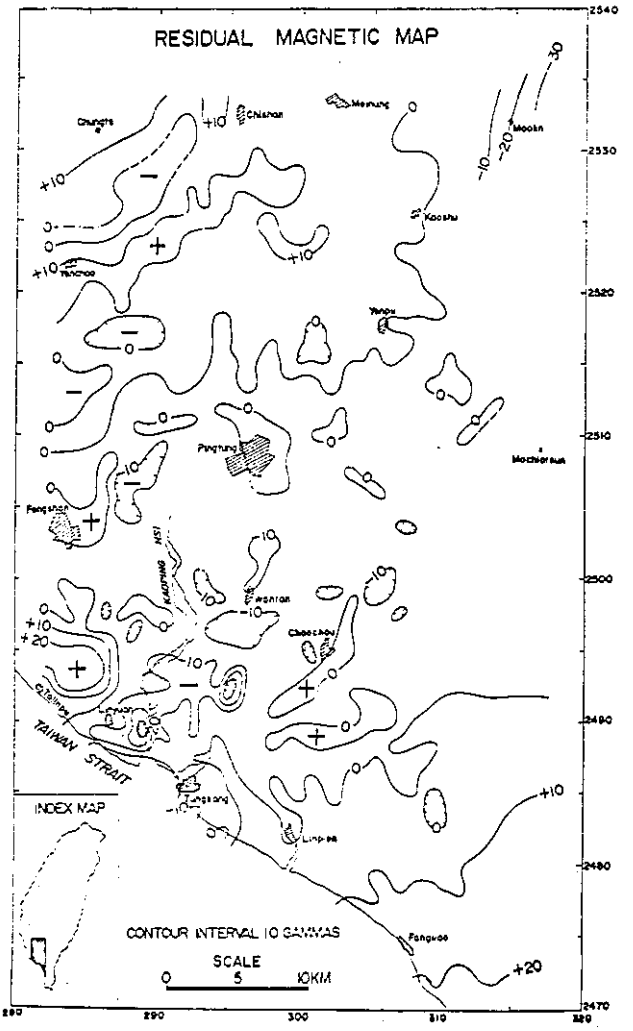

Figure 9. Residual magnetic map of the Pingtung plain.

large quantity of steel constructions in the Linhai[19] industrial district. Besides these small-scale anomalies large-scale anomalies of low amplitude are prominent features recognized in the plain. The central part of the plain has negative anomalies with amplitude of of several gammas, while both the northwestern and southeastern parts have positive anomalies of 10 to 20 gammas. They may be due to deep-seated basement rocks.

The N-S trending Chaochou fault has strong effect on the Bouguer gravity contours as shows in Figure 2, but no clear change of magnetic anomaly values was found in several E-W trending magnetic profiles (see Figure 3) across the fault. In the northeast corner of the plain, the magnetic anomaly data of the profile from Kaoshiu[20] to Maolin shows that the anomaly values decrease rapidly from west to east.

MAGNETIC ANOMALIES REDUCED TO THE POLE AND THE MAGNETIC BASEMENT RELIEF

The shape of the magnetic anomaly depends not only upon the physical dimensions of the causative body, but also on the orientations of the earth's normal total field vector and the magentization vector associated with the body. It makes the job of interpretation a very difficult one indeed. In order to get rid of the influence of magnetic latitude on the anomalies, we can reduce the anomalies to the magnetic pole of the earth.

Bhattacharyya (1965) represented the total intensity anomalies by a double Fourier series expansion in the cosine and sine form. This harmonic expansion of the anomalies makes it possible to evaluate accurately the field reduced to the pole. Whan and Lu (1977) followed the method of Bhattacharyya but expressed the total intensity anomaly at any point in the space as a complex Fourier series

$$T(x, y, z) = \sum_k \sum_m F_{k,m} \exp\{2\pi i (kx + my)/N\} \exp\{2\pi \sqrt{k^2 + m^2}\, z\}$$

where $F_{k,m} = \frac{1}{N^2} \sum \sum T(x, y, o) \exp\{2\pi i (kx + my)/N\}$

where N is the total number of sample points. The rectangular Cartesian coordinates are chosen such that in the plane of observation the x axis points northward and the y axis eastward. The z axis is taken positive vertically downward.

Let

I, D be the inclination and the declination of the local geomagnetic field respectively,

$I_s = 180^\circ - I$,

I_m, D_m be the inclination and the declination of the magnetization vector $\vec{M}$ respectively,

$I_{ms} = 180^\circ - I_m$,

$k' = 2\pi k/N$, $m' = 2\pi m/N$, $P_{mn} = (k'^2 + m'^2)^{1/2}$,

$\phi_1 = \cot I_s (k' \cos D + m' \sin D)$,

$\phi_2 = \cot I_{ms} (k' \cos D_m + m' \sin D_m)$,

G be the gravitational constant

The pseudo-gravity anomaly Vp which can be interpreted as the gravity anomaly produced by an anomalous mass of density $\sigma = |\vec{M}| / G$ and the total intensity magnetic anomaly reduced to the pole Tp are derived to be

$$Vp = \frac{1}{\sin I_{ms} \sin I_s} \sum_k \sum_m F'_{k,m} P_{mn} \exp\{i (k'x + m'y)\} \exp(P_{mn} z)$$

$$Tp = \frac{1}{\sin I_{ms} \sin I_s} \sum_k \sum_m F'_{k,m} P^2_{mn} \exp\{i (k'x + m'y)\} \exp(P_{mn} z)$$

where $F'_{k,m} = \frac{F_{k,m} \{P^2_{mn} - \phi_1 \phi_2 + i P_{mn} (\phi_1 + \phi_2)\}}{(P^2_{mn} + \phi_1^2)(P_{mn} + \phi_2^2)}$

The magnetic basement relief $\Delta h(x, y)$ can be estimated by employing the Bouguer fomula

$$\Delta g(x, y) = 2\pi G \sigma \Delta h(x, y) = 2\pi |\vec{M}| \Delta h(x, y)$$

where $\Delta g\ (x, y)$ is the pseudo-gravity anomaly continued downward to a horizontal plane passing through the center of mass of the magnetized body.

A model composed of two prisms was set up for testing the applicability of the method described above. The dotted lines in Figure 10 indicate the positions of two prisms. The tops of the larger one and the smaller one are at 3 km and 4 km below the observational plane, respectively, and their bases are both at 6 km below the plane. Assuming $I = I_m = 30.4°$, $D = D_m = -1.8°$, and $|\vec{M}| = 180$ gammas, which are the parameters appropriate for the Pingtung plain, the magnetic anomalies generated by these two prismatic magnetized bodies are shown in Figure 10A. Anomalies produced by the same bodies at the north magnetic pole of the earth (with $I = I_m = 90°$, $D = D_m = 0°$, $|\vec{M}| = 180$ gammas) are illustrated in Figure 10B. Then the anomalies shown in Figure 10A are reduced to the pole and the result is shown in Figure 10C. It is clear that Figure 10C is very close to Figure 10B except in the central part of two prisms where the reduced field values are slightly smaller than the actual values. Figure 10D shows the basement relief estimated from the downward continuation of the pseudo-gravity anomalies to 5 km below the observational plane. The positions of the basement high coincide exactly with the locations of the tops of the bodies. But the shape of the basement relief are somewhat distorted due to the sharp discontinuity at the edges of the rectangular bodies.

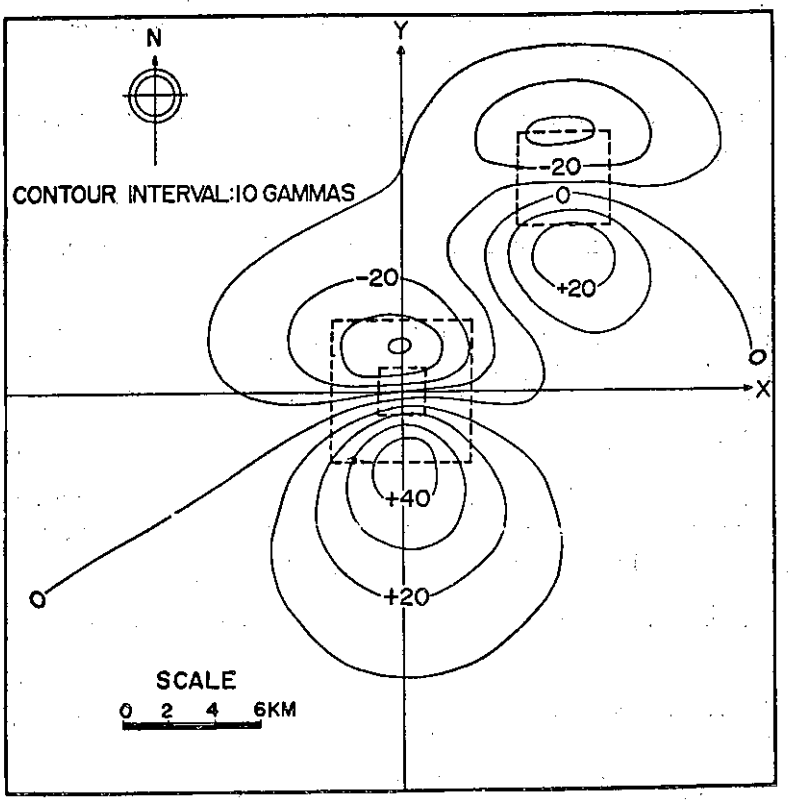

Figure 10A. Magnetic anomalies generated by two prisms with $I=I_m=30.4°$, $D=D_m=-1.8°$.

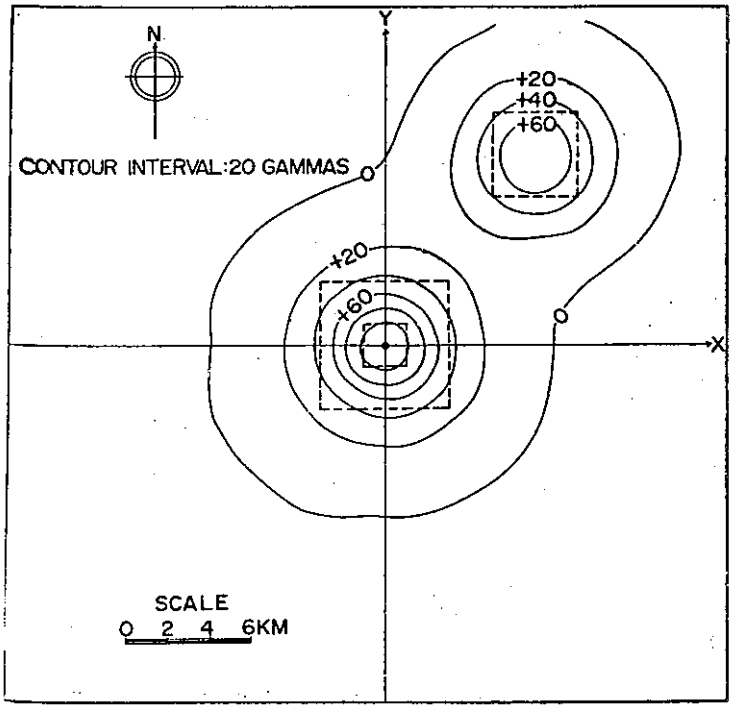

Figure 10B. Magnetic anomalies generated by the same bodies with $I = I_m = 90^\circ$, $D = D_m = 0^\circ$

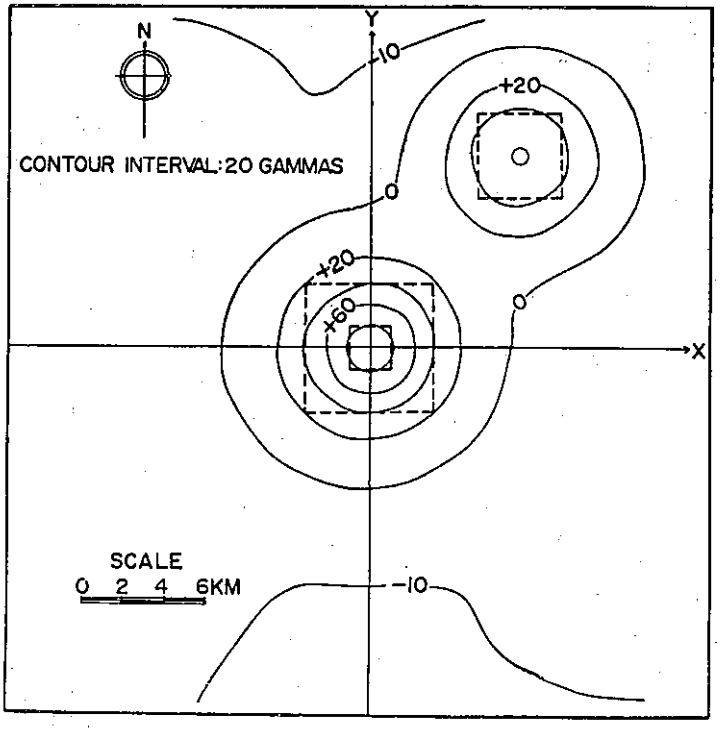

Figure 10C. Magnetic anomalies of Figure 10A reduced to the pole.

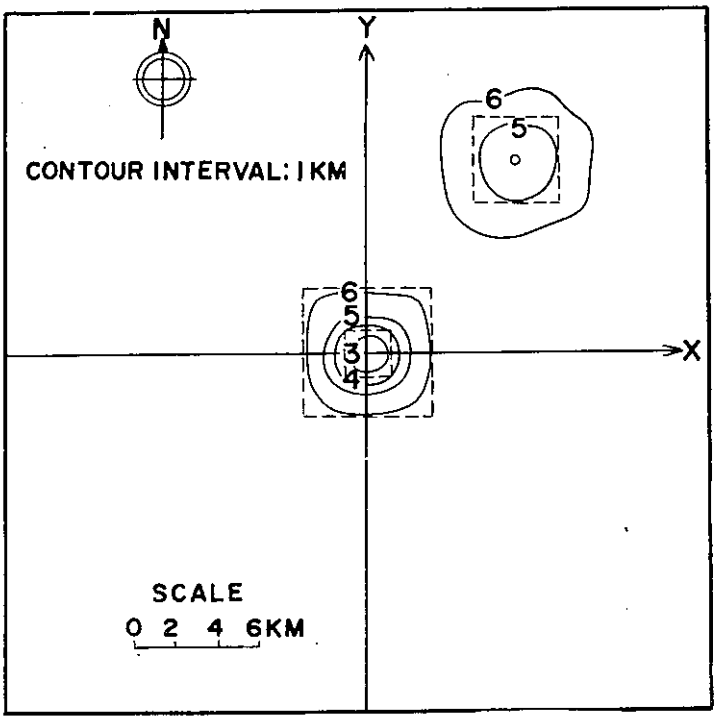

Figure 10D. Magnetic basement relief from the downward continuation to 5 km below the observational plane.

The method of Whan and Lu is then applied to reduce the residual magnetic anomalies of Pingtung plain (Figure 9) to the pole. Since the fast Fourier transform technique has been used, the input data must be equally spaced and the number of data must be $2^L \times 2^L$, where L is a positive integer. For satisfying the requirement of equally spaced input data a grid spacing of 1 km is selected, and the anomaly value at each regular grid point is estimated by weighted average of values at six nearest irregularly spaced data points. Also zeros are added into the input data array to achieve the requirement of $2^6 \times 2^6$ data points.

The magnetic anomalies of the Pingtung plain reduced to the pole with the assumptions of $I = I_m = 30.4°$, $D = D_m = -1.8°$, $\vec{M} = 180$ gammas are contoured in Figure 11. The abrupt decrease of the reduced anomalies at the southeast and the northeast corners of the mapped area may be due to marginal effects. The magnetic basement relief of the plain evaluated from downward continuation of the pseudo-gravity anomalies to 8 km below the surface is shown in Figure 12. With this method of evaluation, the amplitude of basement relief varies inversely with the magnetization contrast. Thus the relief shown in Figure 12 should be modified accordingly if the magnetization data of the basement are available.

The relief of the magnetic basement is generally flat. A gentle magnetic basement high with N-S trending lies between Chaochou and Linpien[21], while a basement low with small amplitude extends northerly from Linyuan[22] to Likang[23]. They do not seem to be related to the subsurface structures inferred by Hsieh (1970) (see Figure 2). The magnetic basement does not necessarily have to agree with the geological basement. In general, the basement is composed of magnetic and non-magnetic parts so that only the magnetic basement or the magnetic part of the basement can be detected by the magnetic survey. It is interesting to note

that the Kaoping Hsi lies directly over the magnetic basement low.

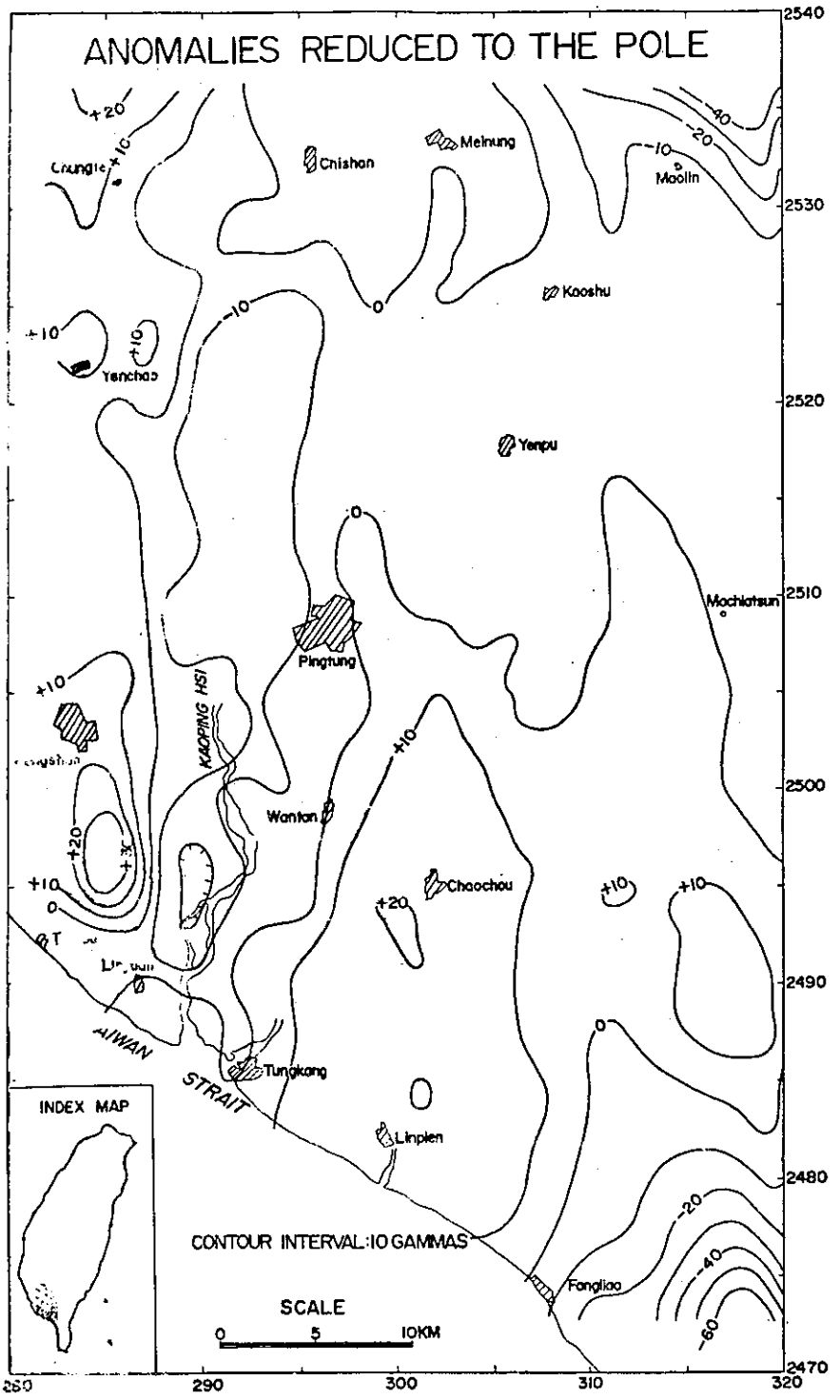

Figure 11. Magnetic anomalies of the Pingtung plain reduced to the pole.

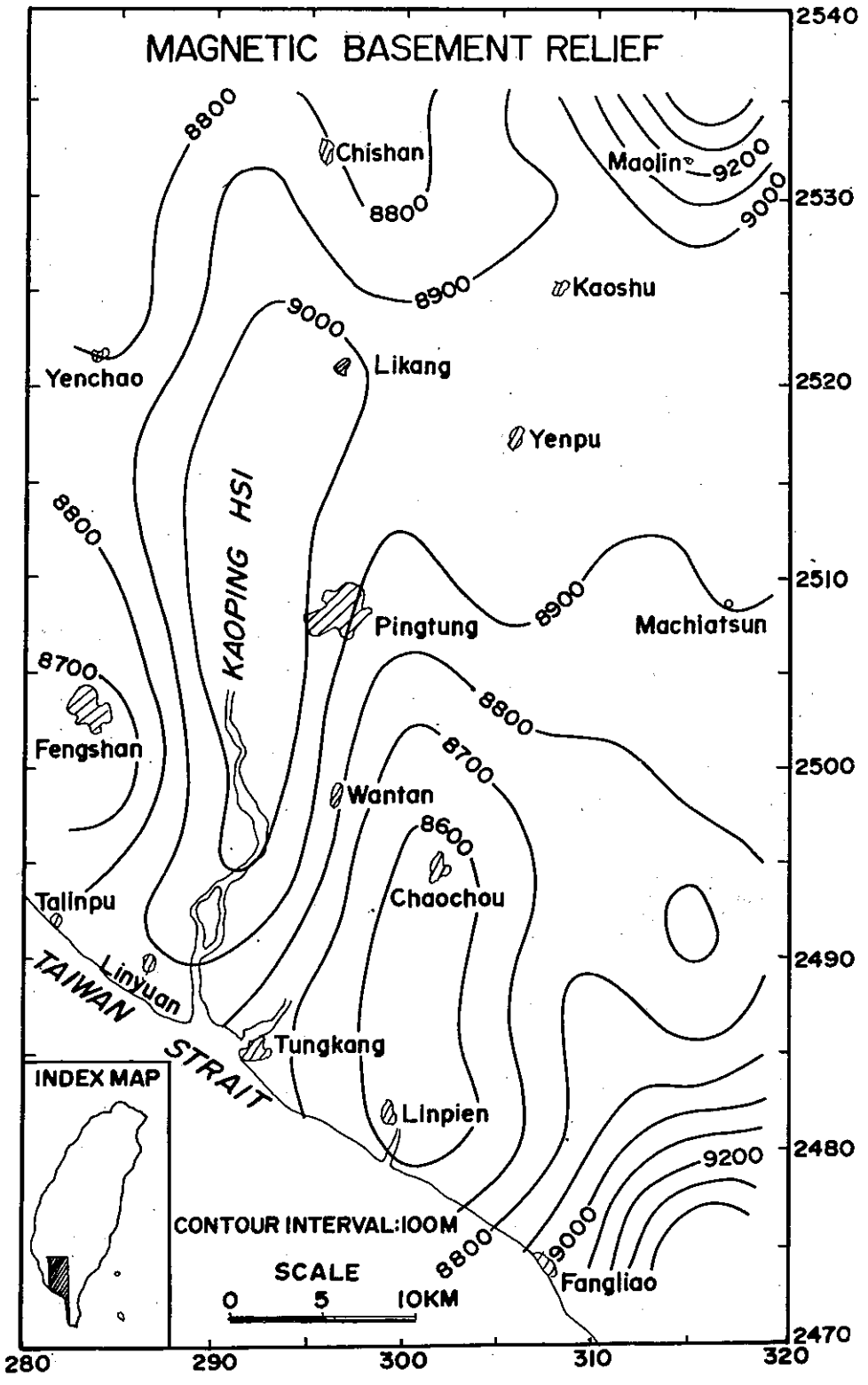

Figure 12. Magnetic basement relief of the Pingtung plain.

CONCLUSIONS

In the magnetic survey conducted in the Pingtung plain no remarkable magnetic anomaly of large amplitude was found. This means that no igneous body exists at shallow depths. There are many magnetic anomalies of small amplitude with an extent of only a few kilometers scattered over the entire plain. They may be caused by local variations of magentic susceptibility of near-surface sedimentary rocks or by the cultural disturbances from nearby towns and industrial districts. Besides these small-scale anomalies, a regional anomaly of low amplitude can be recognized in the plain. It may be due to relief of the deep-seated basement rocks. No significant change of magnetic anomaly values was found in several E-W trending magnetic profiles across the N-S trending Chaochou fault, even though the fault has strong effect on the Bouguer gravity contours.

After comparing the linear secular variation predicted by IGRF 1975 with the observed geomagnetic data at Lunping Observatory, it is concluded that the errors in secular change correction will be within several gammas by using IGRF 1975 to reduce the magnetic survey data in Taiwan region during the period from 1965 to 1973. For magnetic survey data obtained after the epoch 1974.0, an appropriate correction should be made if IGRF 1975 is utilized in reducing those data. In the case of the Pingtung plain the horizontal gradient of the first-degree trend surface of total intensity is slightly different from that of IGRF contours. It is found that the former is more suitable for representing the regional field of the plain than the latter.

The magnetic anomalies of the Pingtung plain are reduced to the pole and by downward continuation through the pseduo-gravity anomalies the magnetic basement relief of the plain is determined. In the calculation it is assumed that the direction of the magnetization vector of the basement is the same as that of the present earth magnetic field because no magnetization data of the basement samples are available. The estimated magnetic basement high lies between Chaochou and Linpien, while a basement low extends northerly from Linyuan to Likang. They are apparently not related to the subsurface structures inferred by Hsieh (1970) based on the gravity data.

ACKNOWLEDGMENTS

We thank our colleagues Messrs. Y.S. Cheng, C.C. Hsu, Y.C. Yang, and D.A. Lee for their assistance in field survey. Thanks are also due to Mr. S.Y. Hwang of National Chunghsin University for his assistance in data reduction. This study was funded by the National Science Council of the Republic of China under Grant no. NSC-68M-0202-02 (01).

REFERENCES

Bhattacharyya, B.K. (1965). Two-dimensional harmonic analysis as a tool for magnetic inter pretation, *Geophysics*, 30, 829-857.

Grant, F.S. and G.F. West (1965). *Interpretation theory in applied geophysics*, McGraw-Hill Book Co., 583 p.

Hsieh, S.H. (1970). Geology and gravity anomalies of the Pingtung plain, Taiwan, *Proc. Geol. Soc. China*, no. 13, 76-89.

Hsu, T.L. (1961). The artesian water system beneath the Pingtung valley, southern Taiwan, *Proc. Geol. Soc. China*, no. 4, 73-81.

Pan, Y.S. (1968). Interpretation and seismic coordination of the Bouguer gravity anomalies obtained in southwestern Taiwan, *Petroleum Geol. Taiwan*, no. 6, 197-207.

Regan, R.D. and J.C. Cain (1975). The use of geomagnetic models in magnetic surveys, *Geophysics*, 40, 621-629.

Whan, W.J. and R.S. Lu (1977). Two applications of Fourier analysis to reduce marine magnetic anomalies in the Taiwan-Luzon region to the pole. *Acta Oceanographic Taiwanica*, no. 7, 32-43.

Institute of Earth Sciences
Academia Sinica
P.O. Box 23-59
Taipei, Taiwan
Republic of China

屏東平原之磁力研究

余水倍　蔡義本

摘　　要

本處於1978年冬完成屏東平原之磁力測勘，測勘面積廣達1400 km^2。兩部靈敏度為1伽瑪之提式質子磁力儀同時用於測定本區之全磁力值。經日變化修正之全磁力值減去一次傾向面值得剩餘磁力值。剩餘磁力圖顯示本區磁力異常之主要特徵有二；一為零散分佈於整個平原振幅小於20伽瑪且涵蓋範圍僅及數公里的局部磁力異常，它們可能是由近地表沉積岩磁化率之局部變化或城鎮及工業區引起的人為磁性干擾所產生的。另一是由深部基岩起伏或其磁性變化導致的低振幅大區域磁力異常。將 IGRF 1975 推算之線性年變化與台灣西北部崙坪觀測站之歷年地磁資比較，我們發現在1965至1973年間實際觀測之年變化與IGRF 1975推算者甚為接近，僅相差數伽瑪。反之，在1974年以後觀測值逐年遞增，與IGRF 1975所預測之遞減趨勢正好相反。因此，在應用IGRF 1975處理台灣地區1974年以後獲得之地磁資料時應作若干修正。此外我們亦發現全磁力之一次傾向面較IGRF等值線更能代表屏東平原之區域性磁力。最後，我們以快速傅氏轉換法將本區之磁力異常轉移至地磁北極，並經由假重力異常以向下延伸法估算屏東平原磁性基盤之起伏。